Effective ionization and dissociation rate coefficients of molecular hydrogen in plasma

Keiji Sawada[a)]
Department of Applied Science, Faculty of Engineering, Shinshu University, Nagano 380, Japan

Takashi Fujimoto
Department of Engineering Science, Faculty of Engineering, Kyoto University, Kyoto 606-01, Japan

(Received 5 December 1994; accepted for publication 22 May 1995)

A simplified collisional-radiative model has been constructed for the system of the ground state, electronically excited stable states, and the ionic state of molecular hydrogen in plasma. Effective rate coefficients have been calculated for production of electrons, molecular ions, protons, and hydrogen atoms from molecular hydrogen. The ratio of the effective ionization rate of molecular hydrogen to the Balmer α photon emission rate and the effective rate coefficients for radiation and energy losses are also presented. © *1995 American Institute of Physics.*

I. INTRODUCTION

Plasma particles in a toroidal fusion device, such as a tokamak, leave the core region across the magnetic-field lines and impinge upon the wall or limiters. A fraction of the incident plasma particles is recycled back as neutral particles. It is a well known fact that the performance of the core plasma is strongly related with the characteristics of the plasma in the outer region. It is therefore essential to understand the transport of the neutral and charged particles in these regions.

Several years ago the present authors proposed a method to determine the atomic hydrogen density, the molecular hydrogen density, and the electron density from the observed atomic line intensities emitted from a plasma which contains atomic and molecular hydrogen as neutral species.[1] This method is based on the fact that the population distribution over the excited atomic levels depends on whether these atoms are produced from atomic hydrogen or molecular hydrogen and on the fact that the population distribution also depends on electron density. They applied this method to a tokamak plasma and found that more than 90% of neutral hydrogen in the outer region was molecular.[2] This finding strongly suggests that the neutral hydrogen released from the container wall or the limiter is predominantly molecular.

Our concern is then the particle balance of hydrogen: molecules which are released from the wall or the limiter and flow into the plasma would also be ionized or dissociated to produce molecular ions, protons, or atoms. These latter particles are also subject to further dissociation, ionization, and the particle transport. The particle balance including the transport is expressed by the following equations:

$$\frac{dn_{\mathrm{H}}}{dt}=-D_{\mathrm{H}}n_{\mathrm{H}}n_e+\underline{P^{\mathrm{H}}_{\mathrm{H}_2}}n_{\mathrm{H}_2}n_e+P^{\mathrm{H}}_{\mathrm{H}_2^+}n_{\mathrm{H}_2^+}n_e+\Gamma^{\mathrm{in}}_{\mathrm{H}}-\Gamma^{\mathrm{out}}_{\mathrm{H}}, \quad (1)$$

$$\frac{dn_{\mathrm{H}_2}}{dt}=-\underline{D_{\mathrm{H}_2}}n_{\mathrm{H}_2}n_e+\Gamma^{\mathrm{in}}_{\mathrm{H}_2}-\Gamma^{\mathrm{out}}_{\mathrm{H}_2}, \quad (2)$$

$$\frac{dn_{\mathrm{H}^+}}{dt}=P^{\mathrm{H}^+}_{\mathrm{H}}n_{\mathrm{H}}n_e+\underline{P^{\mathrm{H}^+}_{\mathrm{H}_2}}n_{\mathrm{H}_2}n_e+P^{\mathrm{H}^+}_{\mathrm{H}_2^+}n_{\mathrm{H}_2^+}n_e+\Gamma^{\mathrm{in}}_{\mathrm{H}^+}-\Gamma^{\mathrm{out}}_{\mathrm{H}^+}, \quad (3)$$

$$\frac{dn_{\mathrm{H}_2^+}}{dt}=-D_{\mathrm{H}_2^+}n_{\mathrm{H}_2^+}n_e+\underline{P^{\mathrm{H}_2^+}_{\mathrm{H}_2}}n_{\mathrm{H}_2}n_e+\Gamma^{\mathrm{in}}_{\mathrm{H}_2^+}-\Gamma^{\mathrm{out}}_{\mathrm{H}_2^+}, \quad (4)$$

$$\frac{dn_e}{dt}=P^{e}_{\mathrm{H}}n_{\mathrm{H}}n_e+\underline{P^{e}_{\mathrm{H}_2}}n_{\mathrm{H}_2}n_e+P^{e}_{\mathrm{H}_2^+}n_{\mathrm{H}_2^+}n_e+\Gamma^{\mathrm{in}}_{e}-\Gamma^{\mathrm{out}}_{e}, \quad (5)$$

where n_{H}, n_{H_2}, n_{H^+}, n_e, and $n_{\mathrm{H}_2^+}$ are, respectively, the densities of hydrogen atoms, molecules, protons, electrons, and molecular ions. Rate coefficients P stand for the effective production rate coefficients; e.g., $P^{\mathrm{H}}_{\mathrm{H}_2}$ is the rate coefficient for production of hydrogen atoms from hydrogen molecules. Coefficients D stand for the effective depletion rate coefficients; e.g., D_{H_2} is the rate coefficient for hydrogen molecules. Γ^{in} and Γ^{out} are, respectively, the flux into and out of a unit volume of the plasma at this location. In Eqs. (1)–(5) we have neglected the recombination terms, e.g., $P^{\mathrm{H}}_{\mathrm{H}^+}n_{\mathrm{H}^+}n_e$, because the plasma of our present interest is a typical example of the ionizing plasma in which recombination processes are insignificant.[3]

In order to investigate the particle balance in plasma as described by Eqs. (1)–(5), the rate coefficients P and D should be known. The cross sections for direct processes, e.g., ionization H_2 $(X^1\Sigma_g^+)\rightarrow\mathrm{H}_2^+(X^2\Sigma_g^+)$ by electron impacts, are well established now. However, since our plasma has finite electron densities, indirect processes, e.g., the ladder-like excitation ionization[3] through Rydberg molecular states, should also be included. In order to assess the importance of these processes, we have constructed a collisional-radiative (CR) model for the system of molecular hydrogen.

A part of the results has already been reported: the effective ionization rate coefficient of molecular hydrogen, $P^{e}_{\mathrm{H}_2}$, in Ref. 4. In that article, however, only a brief account was given of the CR model. The details of the model are explained in Sec. II.

In the following, by using this CR model and the CR model for the system of atomic hydrogen,[1,4] we calculate the effective rate coefficients which are underlined in Eqs. (1)–

[a)]Electronic mail: sawada@phys202.shinshu-u.ac.jp

 0021-8979/95/78(5)/2913/12/$6.00

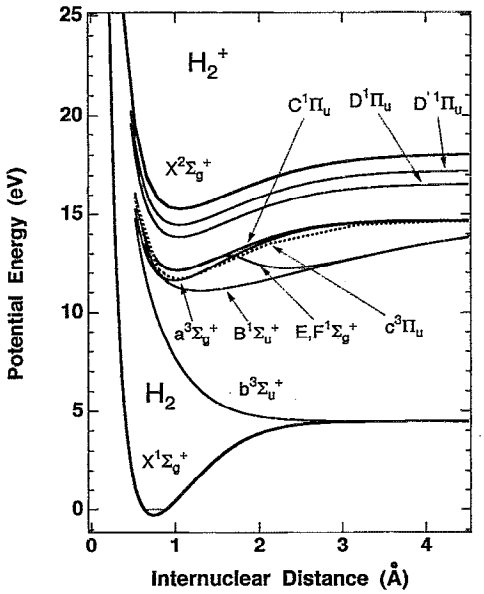

FIG. 1. Some representative electronic states. Potential energy values are taken from Ref. 5.

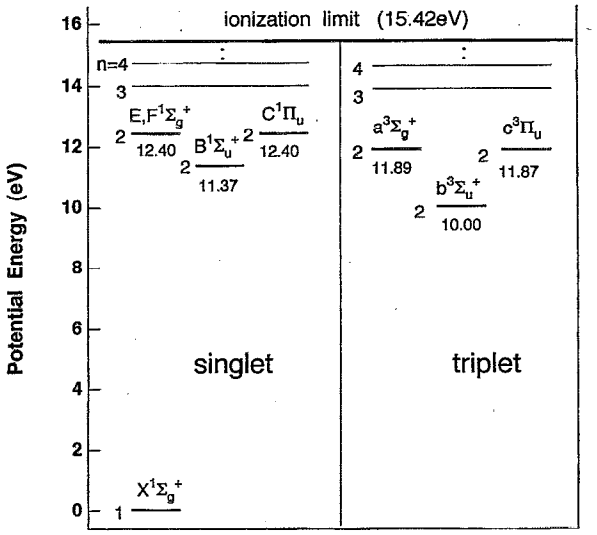

FIG. 2. Simplified energy-level diagram of molecular hydrogen considered in our calculation.

(5). The results are given in Sec. III. The ratio of the effective ionization rate of molecular hydrogen to the Balmer α (Hα) photon emission rate and the effective energy loss rate coefficient from plasma electrons are also presented. Discussions are given in Sec. IV, including effects of vibrational excitation in the ground state. The Appendix gives various data used in our model.

II. COLLISIONAL-RADIATIVE MODEL OF MOLECULAR HYDROGEN

Molecular hydrogen has a number of electronic, vibrational, and rotational states (see Fig. 2 in Ref. 5): Some representative electronic states are shown in Fig. 1. In this study we are primarily interested in the effective dissociation and ionization rates through the stable molecular states rather than in the populations in these states. Thus, we adopt a rather crude approximation: We assume that the initial state of a transition, collisional or radiative, is the ground vibrational-rotational state in the stable electronic state. The validity of this approximation is discussed in Sec. IV. Figure 2 shows the simplified energy level diagram which we adopt. We use n to indicate the principal quantum number of the level in the united-atom limit. For the $n=2$ levels, we consider the singlet states $B^1\Sigma_u^+$, $C^1\Pi_u$, $E,F^1\Sigma_g^+$, and the triplet states $b^3\Sigma_u^+$, $c^3\Pi_u$, $a^3\Sigma_g^+$. For $n\geq 3$, we distinguish singlet and triplet levels. The levels are considered up to $n=28$ in our calculation.

The term values of the $n=2$, 3, and 4 levels are given in Refs. 6, 7, and 8. For $n\geq 5$ levels we use the term value

$$W_n = I_{H_2} - R_H/n^2, \tag{6}$$

where I_{H_2} and R_H are the ionization potential of molecular hydrogen in its ground vibrational-rotational state (15.42 eV) and that of the hydrogen atom (13.6 eV), respectively.

Let p specify a stable molecular state. The time development of the population density of state p is described by the differential equation

$$\frac{dn_{H_2}(p)}{dt} = \sum_{q<p} C_{H_2}(q,p) n_e n_{H_2}(q) - \Bigg[\Bigg(\sum_{q<p} F_{H_2}(p,q) + \sum_{q>p} C_{H_2}(p,q) + S_{H_2}(p)\Bigg) n_e + \sum_{q<p} A_{H_2}(p,q)\Bigg] n_{H_2}(p) + \sum_{q>p} [F_{H_2}(q,p) n_e + A_{H_2}(q,p)] n_{H_2}(q) + [\alpha_{H_2}(p) n_e + \beta_{H_2}(p)] n_{H_2^+} n_e, \tag{7}$$

coupled with similar equations for other states, where $C_{H_2}(p,q)$ and $P_{F_2}(q,p)$ are the excitation rate coefficient by electron impacts from state p to q and its inverse deexcitation rate coefficient, respectively, $A_{H_2}(p,q)$ is the spontaneous transition probability from p to q, $S_{H_2}(p)$ and $\alpha_{H_2}(p)$ are the ionization rate coefficient and the three-body recombination rate coefficient for state p, respectively, and $\beta_{H_2}(p)$ is the radiative recombination rate coefficient. The notation $q<p$ means that level q lies energetically lower than level p. The triplet $b^3\Sigma_u^+$ is a repulsive state. We assume that all the transitions from stable states to this state result in dissociation; we put excitation rate coefficients from this state equal to zero in Eq. (7). All the transitions from stable states to other repulsive states are assumed to autoionize and included in $S_{H_2}(p)$ (see the Appendix).

We assume that excited molecules are not produced starting from the ground- and excited-state atoms and protons. We also ignore transitions due to collisions with atoms, molecules, and ions. The molecular data adopted in our model are summarized in the Appendix.

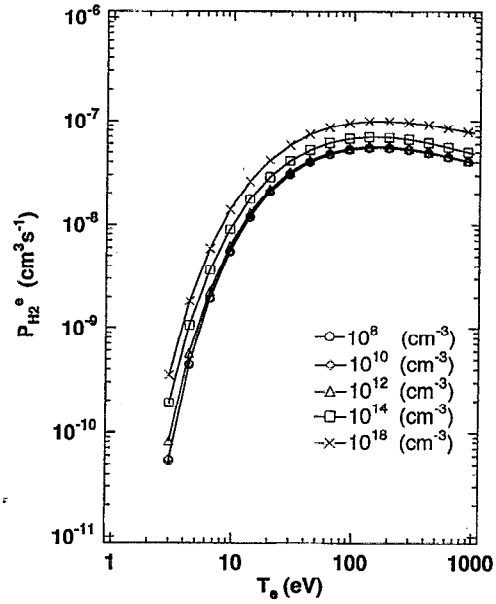

FIG. 3. The effective ionization rate coefficient $P^e_{H_2}$ against electron temperature, with electron density as a parameter.

According to the method of the quasi-steady-state solution,[9–11] Eq. (7) is approximated to zero for all of the excited levels,

$$\frac{dn_{H_2}(p)}{dt}=0, \quad p \text{ is the excited level.} \tag{8}$$

Thus, instead of the coupled differential equations Eq. (7), we have the coupled linear equations, Eq. (8), which contain as parameters n_{H_2} and $n_{H_2^+}$. These equations are readily solved in the form

$$n_{H_2}(p)=R_0^{H_2}(p)n_{H_2^+}n_e+R_1^{H_2}(p)n_{H_2}n_e. \tag{9}$$

Here $R_0^{H_2}(p)$ and $R_1^{H_2}(p)$ may be called the population coefficients and are functions of electron density n_e and temperature T_e.

By using $R_1^{H_2}(p)$ under various plasma conditions we calculate the effective rate coefficients for dissociation and ionization.

III. RESULTS

A. Production of electrons

Figure 3 shows $P^e_{H_2}$ as a function of T_e for several n_e. There are four pathways of ionization from molecular hydrogen. Figure 4 shows the contributions separately from these pathways as functions of n_e. The first is the direct ionization by electron impacts,

path I1:

$$H_2(X^1\Sigma_g^+)+e\rightarrow H_2^+(X^2\Sigma_g^+)+e+e.$$

The cross section is well established.[12,13] The rate coefficient is, of course, independent of n_e.

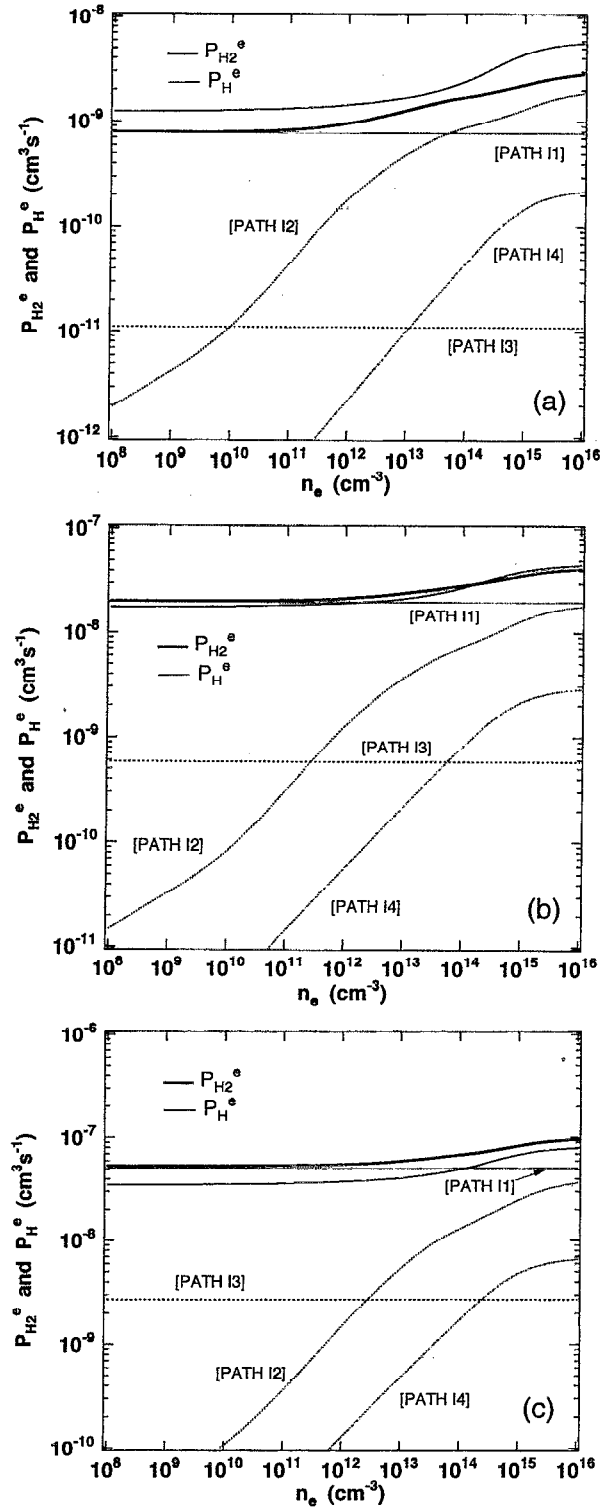

FIG. 4. The ionization rate coefficients through the various pathways (*paths* I1–I4) against the electron density. The effective (total) ionization rate $P^e_{H_2}$ coefficient is shown with the thick curve. The thin curve is the corresponding rate coefficient for atomic hydrogen. (a) T_e=5 eV, (b) T_e=20 eV, (c) T_e=100 eV.

The second is, starting from the ground-state molecule, a stable excited molecule H_2^* is produced. It is further excited (H_2^{**}), and finally ionized to produce a molecular ion,

path I2:

$$H_2(X^1\Sigma_g^+)+e\rightarrow H_2^*+e,$$

$$H_2^*+e\rightarrow\rightarrow H_2^{**}+e,$$

$$H_2^{**}+e\rightarrow H_2^+(X^2\Sigma_g^+)+e+e,$$

where the double arrows stand for multistep, mainly ladder-like, processes.[3] We calculate this contribution by using the CR model developed in Sec. II. The rate coefficient is given as

$$\sum_{p\geqslant 2} S_{H_2}(p)R_1^{H_2}(p)n_e,$$

where $p\geqslant 2$ denotes all the excited levels. It is seen in Fig. 4 that the rate coefficient for this process is strongly dependent on n_e.

The third is dissociative ionization through the unstable molecular hydrogen ion H_2^+ $(X^2\Sigma_u^+)$,

path I3:

$$H_2(X^1\Sigma_g^+)+e\rightarrow H(1s)+H^++e+e.$$

This cross section is given in Refs. 12, 13, and 14, and its rate coefficient is given in Ref. 15; the rate coefficient is independent of n_e.

The fourth is ionization via excited hydrogen atoms H** originating from dissociative excitation of molecular hydrogen,

path I4:

$$H_2(X^1\Sigma_g^+)+e\rightarrow H(1s)+H^*+e,$$

$$H^*+e\rightarrow\rightarrow H^{**}+e,$$

$$H^{**}+e\rightarrow H^++e+e.$$

In the CR model of the hydrogen atom starting from dissociative excitation of molecular hydrogen, the population density of excited level p (the principal quantum number) is given as

$$n(p)=R_2(p)n_{H_2}n_e, \tag{10}$$

where $R_2(p)$ is the population coefficient given in Ref. 1. The contribution from *path* I4 is given as

$$\sum_{p\geqslant 2} S(p)R_2(p)n_e,$$

where $S(p)$ is the ionization rate coefficient of atomic level p. The rate coefficient is dependent on n_e.

Figure 4 shows the rate coefficients of the above four pathways. The overall ionization rate coefficient $P_{H_2}^e$ is shown with the thick curve. It is seen that, under the edge plasma condition of electron density of $n_e\leqslant 10^{13}$ cm^{-3}, the dominant ionization pathway is *path* I1. The reason for the increase in the contributions from *path* I2 and *path* I4 with an increase in n_e is that the population kinetics of excited molecules and atoms changes from the corona phase (in the case of the atom) or its equivalent (molecules) to the ladder-like excitation-ionization phase.[3] In Fig. 4 the corresponding quantity for atomic hydrogen P_H^e $(=S_{CR})$ is also shown for comparison.

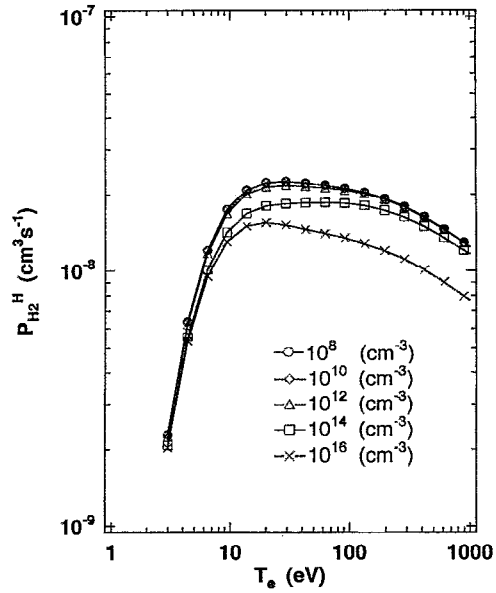

FIG. 5. The effective production rate coefficient $P_{H_2}^H$ of atomic hydrogen by dissociation of molecular hydrogen against electron temperature.

B. Production of atoms—Dissociation

The production rate coefficient $P_{H_2}^H$ is shown in Fig. 5 as a function of T_e for several n_e and its breakdown in Fig. 6. There are five pathways of production of atomic hydrogen. The first is the direct excitation from the ground state to the repulsive level $H_2(b^3\Sigma_u^+)$ by electron impacts,

path H1:

$$H_2(X^1\Sigma_g^+)+e\rightarrow H_2(b^3\Sigma_u^+)+e,$$

$$H_2(b^3\Sigma_u^+)\rightarrow H(1s)+H(1s).$$

The cross section is well established[6,7,16–23] [as shown in Fig. 15(d), below]. The rate coefficient in Fig. 6 is, of course, independent of n_e.

The second is, a ground-state molecule is excited to a stable excited molecule H_2^* by electron impacts. This molecule may further be excited or deexcited to other stable states H_2^{**} by collisional and radiative processes, and finally reaches $H_2(b^3\Sigma_u^+)$,

path H2:

$$H_2(X^1\Sigma_g^+)+e\rightarrow H_2^*+e,$$

$$H_2^{**}\rightarrow\rightarrow H_2(b^3\Sigma_u^+),$$

$$H_2(b^3\Sigma_u^+)\rightarrow H(1s)+H(1s).$$

Here the double arrows denote a sequence of collisional and radiative processes. For the evaluation of the effective rate coefficient for this series of processes, the CR model of molecular hydrogen is used. The contribution from *path* H2 is given as

$$\sum_{p\geqslant 2}[A_{H_2}(p,b^3\Sigma_u^+)+F_{H_2}(p,b^3\Sigma_u^+)n_e]R_1^{H_2}(p).$$

The result is shown in Fig. 6.

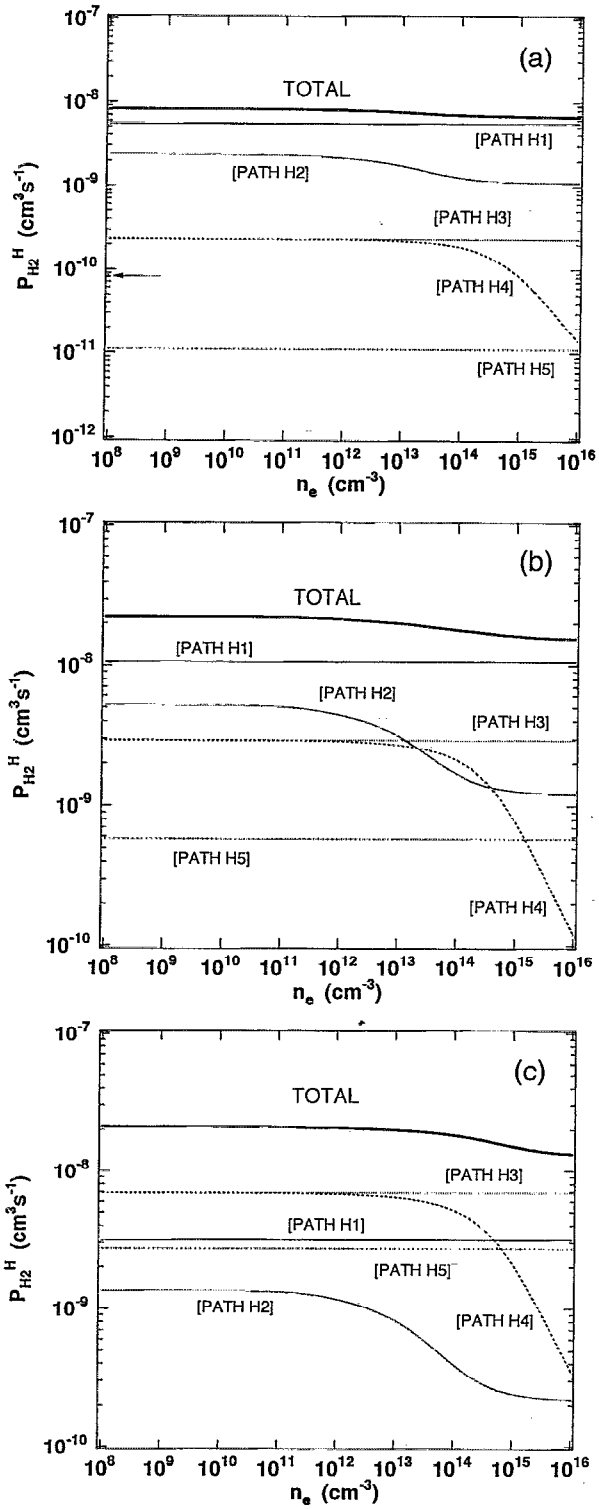

FIG. 6. The production rate coefficients through the various pathways (*paths* H1–H5) against the electron density. The effective (total) production rate coefficient $P_{H_2}^H$ is shown with the thick curve. (a) T_e=5 eV (the arrow indicates the contribution from the vibrationally excited levels of the electronic ground state), (b) T_e=20 eV, (c) T_e=100 eV.

The third is a dissociative excitation process which accompanies the production of excited atomic hydrogen H*,

path H3:

$$H_2(X^1\Sigma_g^+)+e\rightarrow H(1s)+H^*+e.$$

The cross section of the production of the individual excited levels has been discussed in detail in Ref. 4. For the cross section for *path* H3, we employ the sum of the cross sections for production of all of the excited levels (see Fig. 1 of Ref. 4). *Path* H3 is independent of n_e in Fig. 6.

The fourth is the excited atom produced in path H3 is further excited or deexcited by collisional and radiative processes, and finally reaches the ground state,

path H4:

$$H_2(X^1\Sigma_g^+)+e\rightarrow H(1s)+H^*+e,$$

$$H^*\rightarrow\rightarrow H(1s).$$

The contribution from *path* H4 to the dissociation rate coefficient is given as

$$\sum_{p\geq 2}[A(p,1)+F(p,1)n_e]R_2(p),$$

where $A(p,1)$ and $F(p,1)$ are the spontaneous transition probability and the deexcitation rate coefficient for atomic hydrogen $p\rightarrow 1$. The population coefficient $R_2(p)$ has already been calculated.[4] Both the contributions from *path* H3 and *path* H4 are equal in the low-density limit because almost all the produced excited atoms eventually decay radiatively to the ground state without being ionized. Under the edge plasma condition of electron density of $n_e\leqslant 10^{13}$ cm^{-3}, this is almost the case.

With an increase in n_e, the contributions from *path* H2 and *path* H4 decrease. The reason is that with the increase in n_e population kinetics of both the atomic hydrogen and molecular hydrogen changes from the corona phase to the ladderlike excitation-ionization phase.

The fifth is dissociative ionization through the repulsive molecular state,

path H5:

$$H_2+e\rightarrow H(1s)+H^++e+e.$$

This is the same process as *path* I3. This is, of course, independent of n_e.

Figure 6 shows the overall production rate coefficient $P_{H_2}^H$ with the thick curve. As is seen in Fig. 6(c), all the contributions from *paths* H1–H5 can be of the same order of magnitude.

C. Other effective rate coefficients

Figure 7 shows $P_{H_2}^{H_2^+}$, which is the sum of the rate coefficients for *paths* I1 and I2. Figure 8 shows $P_{H_2}^{H^+}$, which is the sum of those for *paths* I3 and I4. Figure 9 shows D_{H_2}, which is the sum of those for *paths* I1, I2, I3, H1, H2, H3, and H5.

D. Ionization rate of molecular hydrogen and Hα line intensity

In toroidal plasma research the amount of the neutral particle influx is sometimes evaluated from the observed Hα line intensity. This technique is based on the assumption that

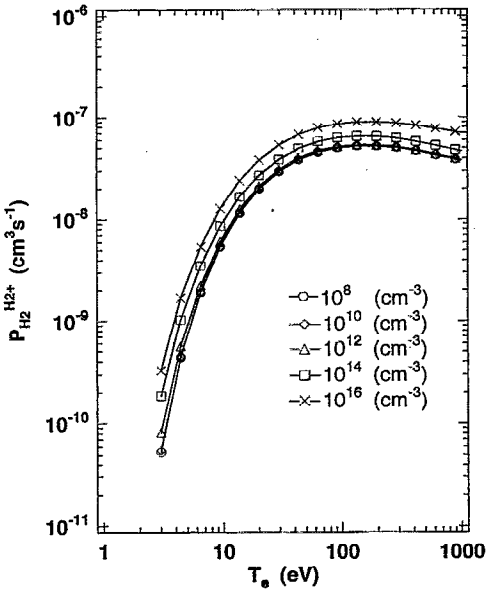

FIG. 7. The effective production rate coefficient of molecular hydrogen ions.

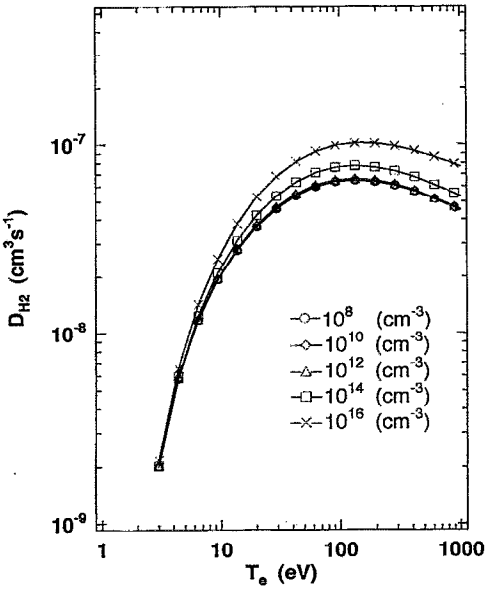

FIG. 9. The effective depletion rate coefficient of molecular hydrogen.

the recycled neutral hydrogen is atomic;[24] however, as mentioned above, Hα photons could also be emitted by the excited atoms that originate from molecular hydrogen. In Fig. 10 the ratio of the effective ionization rate of molecular hydrogen to the Hα photon emission rate is shown,

$$P^e_{H_2} n_{H_2} n_e / A(3,2) R_2(3) n_{H_2} n_e ,$$

where $A(3,2)$ is the spontaneous transition probability of atomic hydrogen $p=3\rightarrow 2$. This figure also contains the corresponding quantity for atomic hydrogen,

$$P^e_H n_H n_e / A(3,2) R_1(3) n_H n_e .$$

It is obvious that the proportional factor for the molecule is more than ten times that for the atom. This is mainly due to the difference in the magnitudes of the cross sections for dissociative excitation and excitation (see Fig. 1 in Ref. 4).

E. Effective energy-loss rate coefficient

Figure 11 shows the effective energy-loss rate coefficient from plasma electrons,

$$\sum_{p\geq 1} \sum_{q>p} [n_{H_2}(p) C_{H_2}(p,q) - n_{H_2}(q) F_{H_2}(q,p)] \times n_e E_{H_2}(p,q) / n_{H_2}(1) n_e + \sum_{p\geq 1} n_{H_2}(p) S_{H_2}(p) n_e E_{H_2}(p) / n_{H_2}(1) n_e ,$$

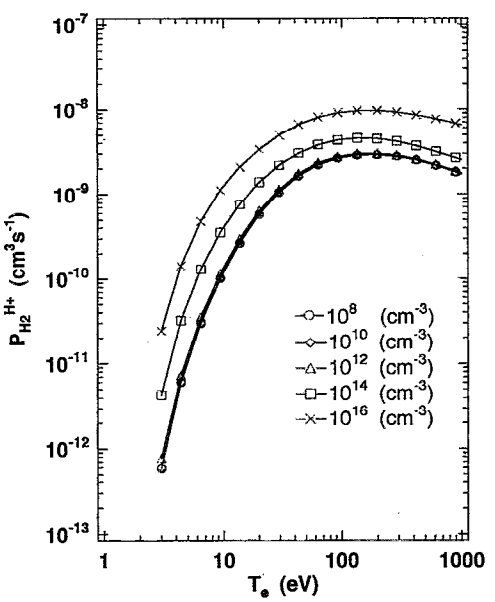

FIG. 8. The effective production rate coefficient of protons.

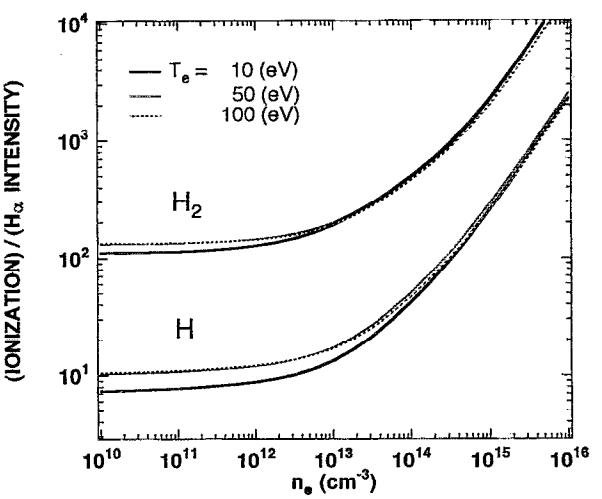

FIG. 10. The ratio of the number of ionization events to the photon number of the Hα emission originating from molecular hydrogen against electron density for several electron temperatures (upper curves denoted by H_2). Also shown is the corresponding quantity for atomic hydrogen (lower curves denoted by H). This figure is the same as Fig. 5 of Ref. 4.

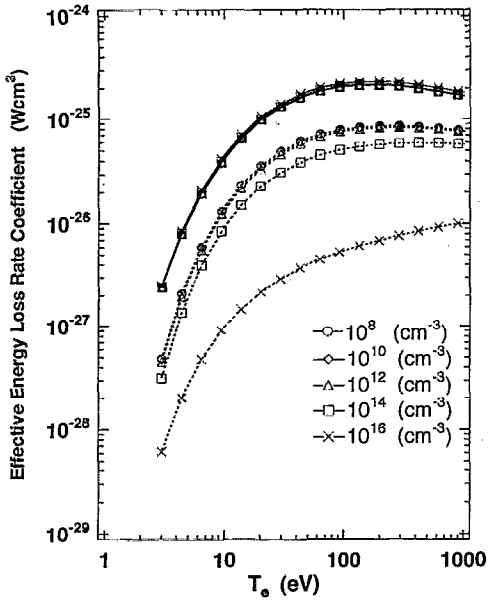

FIG. 11. Energy loss from plasma electrons (solid curves) and radiation loss from plasma (dashed curves) vs electron temperature with the electron density as a parameter.

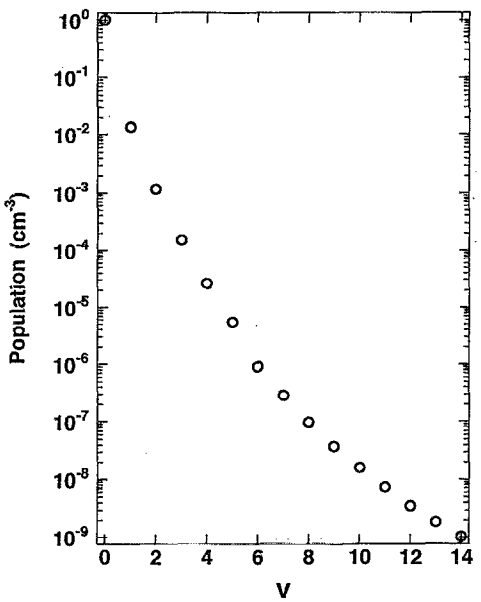

FIG. 12. Relative population of the vibrational levels of the electronic ground state at T_e=5 eV.

where $E_{H_2}(p,q)$ and $E_{H_2}(p)$ are, respectively, the energy difference between level p and q and the ionization energy of molecular hydrogen. In Fig. 11 the radiation loss,

$$\sum_{p\geq 1}\sum_{q>p} n_{H_2}(q)A_{H_2}(q,p)E_{H_2}(p,q)/n_{H_2}(1)n_e,$$

is also shown.

IV. DISCUSSION

We have assumed that the initial state of a transition, collisional or radiative, is the ground vibrational-rotational state in an electronic state. This is because it is impractical to construct a complete CR model including the vibrationally rotationally excited states because the data of the collisional-radiative processes concerning the vibrational-rotational molecular states are scanty. The only exception is the electronic ground state. We have information of the vibrational excitation and of the collisional and radiative transitions concerning the vibrationally excited states. We now examine the effect of vibrational level excitation on the effective ionization rate coefficient $P^e_{H_2}$ and on the effective dissociation rate coefficient $P^H_{H_2}$.

Two processes are identified for excitation of the vibrational levels by electron impacts,[25,26]

(a) $H_2(v)+e\rightarrow H_2^-\rightarrow H_2(w)+e,$

(b) $H_2(v=0)+e\rightarrow H_2(B^1\Sigma_u^+, C^1\Pi_u)+e$
$\rightarrow H_2(w)+e+h\nu.$

For lower electron impact energy ($E<12$ eV), process (a) is dominant,[27] and for higher electron impact energy ($E>12$ eV), process (b) is dominant.[28] We consider the two energy regions separately.

First we consider the low-energy region ($E<12$ eV). The population distribution over the vibrational levels is a result of excitation and deexcitation among the vibrational levels (a), together with excitation to a vibrational continuum and to $b^3\Sigma_u^+$ from the vibrational levels. Excitation to higher electronic levels except $b^3\Sigma_u^+$ is negligible.[29] We have constructed a CR model for the 15 vibrational levels of the electronic ground state. The cross section for process (a) is calculated in Ref. 27 for $v,w=0-5$, levels at the impact electron energy of 6 and 8 eV. We extrapolate them to $v,w=0-14$. We assume the energy dependence of the cross sections to be the same as that for 0–1 in Ref. 27. The cross section for excitation from $v=14$ to the vibrational continuum is assumed to be the same as the excitation cross section from $v=0$ to $v=1$. The excitation cross section from $v=0-14$ to $b^3\Sigma_u^+$ is given in Refs. 30 and 31. Figure 12 shows the population of the vibrational levels for T_e=5 eV as calculated on the assumption that the molecular hydrogen is initially produced in the $v=0$ level. The populations of the excited vibrational levels are much smaller than that of the ground vibrational state. The effective production rate coefficient through the excited vibrational levels at T_e=5 eV is shown in Fig. 6(a) with the arrow. This quantity should be added to that of *path* H1. It is concluded that the contribution from the vibrationally excited levels to dissociation is negligible compared with that from the ground vibrational state.

Next we consider the high-energy region ($E>12$ eV). We modify our CR model: The electronic ground state has the vibrational ground state and one excited level that represents all the vibrationally excited levels. In this model, we use for the representative level the averaged cross section or the spontaneous transition probability over the vibrationally

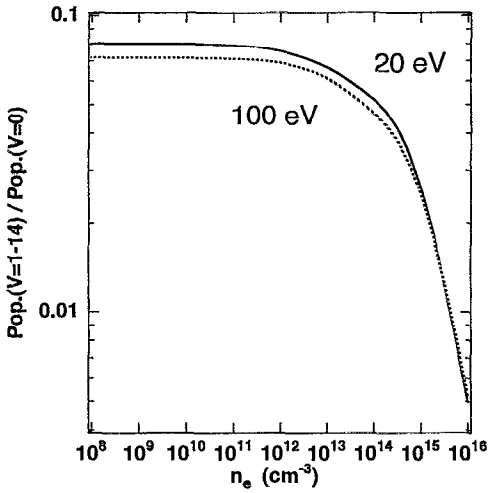

FIG. 13. Ratio of the population of the representative vibrationally excited level to that of the ground state.

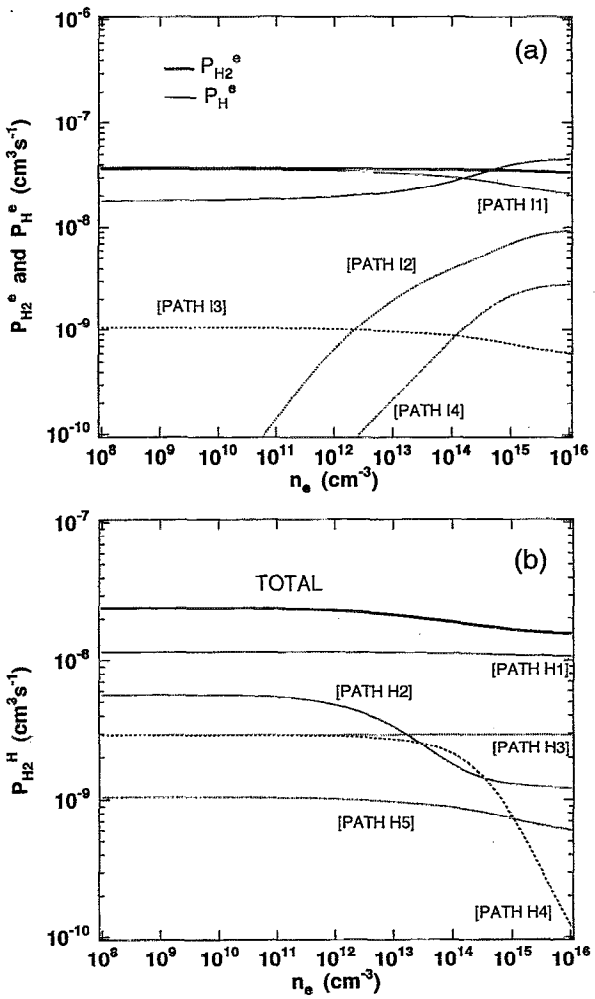

FIG. 14. The result of calculation for effective rate coefficients at T_e=20 eV, where excitation to the vibrationally excited level is taken into account. (a) $P^e_{H_2}$, (b) $P^H_{H_2}$.

excited levels. Excitation cross sections from the vibrationally excited levels to $b^3\Sigma_u^+$ are given in Ref. 32. Their magnitudes are nearly the same as that from the ground vibrational state. Excitation cross sections to $B^1\Sigma_u^+$ and $C\ ^1\Pi_u$ are given in Refs. 33 and 34. The cross section averaged over the excited vibrational levels is approximately twice that for the ground vibrational state. Direct ionization cross sections from the excited levels are given in Refs. 35 and 36. Dissociative ionization cross sections from these levels are given in Ref. 37. Spontaneous transition probabilities from $B^1\Sigma_u^+$ and $C^1\Pi_u$ to each vibrational level of the electronic ground state are given in Ref. 38. The sum of the spontaneous transition probability to all the excited levels is one or two orders larger than that to the vibrational ground state. For the higher electronic excited levels having principal quantum number $n \geqslant 3$, cross sections and spontaneous transition probability to and from the vibrationally excited levels are not known. We estimate them from the values for $n=2$: For $n \geqslant 3$ we approximate the excitation cross section from the vibrationally excited level to the singlet states is two times larger than those from the ground state. For the triplet state, we approximate them to be the same as those from the ground state. For the ionization cross section of the vibrationally excited level, we approximate it to be ten times larger than that from the ground state. Spontaneous transition probabilities from the singlet states to the excited vibrational level[38] are approximated to be one hundred times those to the ground vibrational state. Figure 13 shows the result of the calculation: The ratio of the population of the representative vibrationally excited level to that of the ground state is given as a function of n_e. The effective ionization rate coefficient $P^e_{H_2}$ at T_e=20 eV is shown in Fig. 14(a) which corresponds to Fig. 4(b). In the low electron density region, the rate coefficient is two times larger than that for which vibrationally excited levels are neglected. The effective production rate coefficient $P^H_{H_2}$ is shown in Fig. 14(b), which corresponds to Fig. 6(b). Only a small modification is seen.

As described in detail in the Appendix, we have reasonably reliable molecular data concerning the ground state; however, the data of the processes between the excited states are quite insufficient, and we have made approximations or even assumptions. When possible, we compared the results of different assumptions. For instance, for collision cross sections between the singlet $B^1\Sigma_u^+$, $C^1\Pi_u$ and $E,F^1\Sigma_g^+$ levels as well as between the triplet $b^3\Sigma_u^+$, $c^3\Pi_u$, and $a\ ^3\Sigma_g^+$ levels, we adopted cross sections on the basis of their resemblance to the $p_{1/2}$, $p_{3/2}$, and $s_{1/2}$ levels of atomic hydrogen and compared the result with the present one. We found a very small change.

Although we expect that possible errors in the data employed in the present calculation would not lead to a substantial error in the calculated rate coefficients, we hope, in future, to have reliable data for these processes.

Throughout the present study we ignored transitions due to collisions by atoms, ions, or molecules. For plasmas with a low ionization degree our assumption may not be valid. Vibrational excitation and deexcitation especially could be affected substantially by these collisions.

In this article we do not treat processes starting from the molecular hydrogen ion H_2^+. In actual plasmas contributions

TABLE I. The spontaneous transition probabilities.

Transition	A coefficient (10^9 s^{-1})	Ref.
$B^1\Sigma_u^+ \rightarrow X^1\Sigma_g^+$	1.87	38,39
$C\ ^1\Pi_u \rightarrow X^1\Sigma_g^+$	1.18	38,39
$E,F^1\Sigma_g^+ \rightarrow B^1\Sigma_u^+$	0.0067	40
$a^3\Sigma_g^+ \rightarrow b^3\Sigma_u^+$	0.091	41

from H_2^+ to production of the excited- and the ground-state atoms may not be ignored. These processes can even be more important in divertor plasmas which have higher densities and lower temperatures. However, atomic data on various processes starting from the molecular ion are so scanty that it is impractical to evaluate quantities similar to those presented here for H_2. It is strongly hoped that the cross sections for the processes concerned will become available in the near future.

ACKNOWLEDGMENTS

This work is a part of the joint research program on the WT-3 tokamak, Department of Physics, Kyoto University. The authors would like to thank Professor H. Takagi for giving us information on the transition probabilities of molecular hydrogen. This work is partly supported by the Fellowship of the Japan Society for the Promotion of Science for Japanese Junior Scientists.

APPENDIX: MOLECULAR DATA USED IN THE COLLISIONAL-RADIATIVE MODEL

1. Spontaneous transition probabilities

The spontaneous transition probabilities are taken from Refs. 38–41, and the values are listed in Table I. These values are for transitions from the ground vibrational level ($v'=0$) to all of the vibrational levels of the final state. Except for Table I, the transition probabilities are not available from literature. For other transitions we estimate these values from those for atomic hydrogen,[42] where the difference in the statistical weights of the levels is taken into account.

2. Excitation and deexcitation by electron impacts

a. Excitation from the ground state

The excitation cross sections from the ground state to the singlet states $B^1\Sigma_u^+$, $C^1\Pi_u$, $E,F^1\Sigma_g^+$ and to the triplet states $b^3\Sigma_u^+$, $c^3\Pi_u$, $a^3\Sigma_g^+$ are studied by many workers[6,7,15–23,43–54] (see Table II). The calculations listed in Table II give the total cross section for the transitions from the ground vibrational level ($v''=0$) to all the vibrational levels of the upper state. Figure 15 shows examples of these cross sections, where we have adopted the corrections proposed in Refs. 54 and 55; we have multiplied the cross sections in Refs. 44, 45, and 49 by 0.62 correcting for the sensitivity of the detector.

TABLE II. The references for the excitation cross sections from the ground state to the singlet $B^1\Sigma_u^+$, $C^1\Pi_u$, $E,F^1\Sigma_g^+$ and the triplet $a^3\Sigma_g^+$, $b^3\Sigma_u^+$, $c^3\Pi_u$ states.

State	Review	Experiment	Calculation
$B^1\Sigma_u^+$	6,15	43,44,45,46,47,54	7,17,50,52
$C^1\Pi_u$	6,15	44,45,46,47,48,49,54	50,51
$E,F^1\Sigma_g^+$	6,15		51
$a^3\Sigma_g^+$	6	47	7,18,19,53
$b^3\Sigma_u^+$	6	16	7,17,18,19,20,21,22,23
$c^3\Pi_u$	6	47	7,18,19,51

We fit the cross sections by using the formula given in Ref. 6,

$$\sigma = q_0 A/W^2 (W/E)^{\Omega}\Phi,$$
$$\Phi = [1-(W/E)]^{\nu} \quad \text{(singlet)}, \qquad \text{(A1)}$$
$$1-(W/E)^{\gamma} \quad \text{(triplet)},$$

where q_0 is 6.514×10^{-14} cm^2 eV^2, W and E are the ionization potential and the impact energy, respectively, and A, Ω, γ, and ν are the adjustable parameters. We primarily rely on the experimental data. Results of fitting are shown in Fig. 15 and the parameter values are given in Table III. We use in our calculation the cross section in this analytical approximation. For excitation from the ground state to the $n=3$ levels, there is no theoretical nor experimental cross section. We adopt the formula given in Ref. 6 and multiply the original value by 1.5; this modification is based on the consideration of the continuation property of the cross section against a change of n.

Because there is no cross section data available for $n\geqslant4$ levels, we estimate them by following the method proposed in Ref. 56. We concentrate our attention on the energy range very close to the ionization threshold. For the purpose of determining the cross section at the threshold, we approximate the excitation cross section to be constant ($\sigma_{1,n}=\sigma_0\propto n^{-3}$) and the ionization cross section to be a linear function [$\sigma_{\text{ion}}=\alpha(E-E_{\text{th}})$], where E_{th} is the threshold energy for ionization to a particular vibrational level. We now assume smooth continuation from excitation of the Rydberg states across the ionization limit to ionization. Then it is straightforward to derive the relationship

$$\alpha=\sigma_0/(2R_{\text{H}}/n^3). \qquad \text{(A2)}$$

The above discussion holds for each vibrational level. Figure 16 illustrates the $v=0$ level of the molecular ion and the corresponding $v=0$ level of the Rydberg molecular state, in this case with $n=4$ taken as an example. Reference 57 gives the slope of the ionization cross section for $v=0$ to be 5.1×10^{-19} cm^2/eV, and Eq. (A2) gives the threshold cross section of $1.39\times10^{-17}/n^3$ cm^2. The actual shape, or the energy dependence of the excitation cross section, is assumed to be the same as that of atomic hydrogen ($1\rightarrow n$),[42] and we multiply the latter cross section so that its threshold cross section becomes equal to the above value. A similar procedure is followed for $v=1,2,....,6$ levels on the basis of the slope of the cross section given in Ref. 57. It is noted here that if the level energy of the excited vibrational level exceeds that of the ground vibrational state of the molecular hydrogen ion ($v>4$ in the case of $n=4$), the excited molecule autoionizes quickly.[58,59] We then sum the cross sections for nonautoionizing vibrational levels ($v=0$, 1, 2, and 3 for

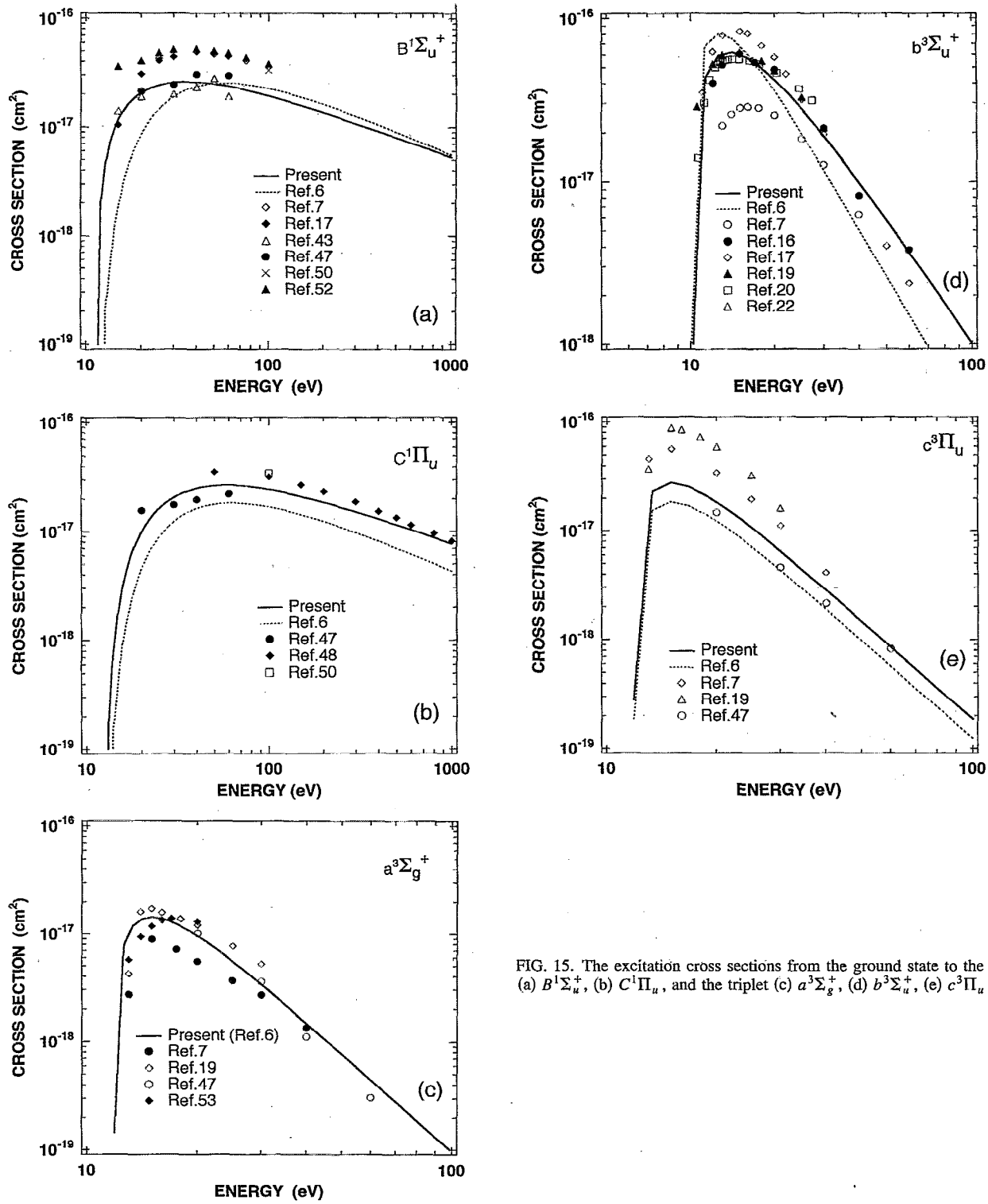

FIG. 15. The excitation cross sections from the ground state to the singlet (a) $B^1\Sigma_u^+$, (b) $C^1\Pi_u$, and the triplet (c) $a^3\Sigma_g^+$, (d) $b^3\Sigma_u^+$, (e) $c^3\Pi_u$ levels.

$n=4$) for the excitation cross section. Table IV shows the vibrational quantum numbers of the nonautoionizing levels and the effective multiplication factor for the excitation cross section. The resulting autoionization cross section derived on our assumption is consistent with the experimental autoionization cross section in Ref. 57. We divide the rate coefficients determined by the above method into the singlet and the triplet levels by using the ratio of the rate coefficient for $n=3$,

$$\text{singlet/triplet} = 0.25 T_e^{1.45} \quad (T_e \text{ in eV}). \tag{A3}$$

b. Excitation between excited levels

There are few reports of the excitation cross sections between the excited levels. For excitation rate coefficient

TABLE III. Parameters in Eq. (A1) for $B^1\Sigma_u^+$, $C^1\Pi_u$, $b^3\Sigma_u^+$, and $c^3\Pi_u$.

	A	Ω	ν	γ
$B^1\Sigma_u^+$	0.173	0.623	1.30	
$C^1\Pi_u$	0.285	0.623	2.27	
$b^3\Sigma_u^+$	1.073	2.765		0.757
$c^3\Pi_u$	0.240	3.0		3.0

TABLE IV. Nonautoionizing vibrational levels and multiplication factor for excitation cross section for the $n \geq 4$ levels.

n	4	5	6	7	≥ 8
v	0–3	0–2	0–1	0–1	0
Factor	0.909	0.665	0.390	0.390	0.140

from $B^1\Sigma_u^+$ to $E,F^1\Sigma_g^+$, we use a formula for the Bethe limit using the oscillator strength which is derived from the corresponding transition probability. We assume that the singlet $E,F^1\Sigma_g^+$ and $C^1\Pi_u$ levels, as well as the triplet $a^3\Sigma_g^+$ and $c^3\Pi_u$ levels, have some resemblance to the $2s$ and $2p$ levels of atomic hydrogen, respectively. For excitation rate coefficients between these levels, we use the Born cross sections for corresponding atomic hydrogen transitions. We approximate excitation cross section from $B^1\Sigma_u^+$ to $C\ ^1\Pi_u$ to be zero because the transition is optically forbidden.

We use the excitation cross section of atomic hydrogen[42] for other transitions of molecular hydrogen.

Deexcitation rate coefficients for both the singlet and triplet levels are derived from the excitation rate coefficients by the principle of detailed balance.

3. Ionization by electron impacts

The ionization cross section from the ground state is given in Refs. 12, 13, and 57. There are no data available for cross sections from excited levels. We estimate them as follows. Ionization consists of two processes: One is the direct ionization producing a molecular hydrogen ion, and another is the indirect process; the molecule is first excited to one of the repulsive Rydberg states, and on its way to dissociate it autoionizes resulting in a molecular ion. We assume that the cross section for the direct process is the same as the corresponding cross section of atomic hydrogen, and we use the semiempirical formula[42] for atoms. For the indirect process the excitation to the repulsive states may be regarded as the excitation of the inner $1s$ electron to $2p$. We then assume the excitation cross section to be given by the cross section for dissociation.

$$H_2^+(X^2\Sigma_g^+)+e \rightarrow H+H^++e,$$

through the repulsive excited state as determined in Refs. 60 and 61. We assume the autoionization probability to be high so that all the excitation results in ionization. This assumption is justified in the following. *Path* H3 is the dissociation process in which a molecule starts from the ground state and after the excitation to the repulsive state it has survived the autoionization. If we assume the excitation cross section from the ground state to the repulsive level to be the same as the atomic excitation cross section from the ground state to the corresponding excited level, it is concluded, from the comparison of this cross section with that of *path* H3 or Fig. 1 of Ref. 4, that more than 90% of the molecules excited to repulsive levels autoionize. This conclusion is consistent with the autoionization probability which is measured in Refs. 62 and 63.

From the description above, it might be assumed that we have neglected processes through the excited molecular ion state, e.g.,

$$H_2(X^1\Sigma_g^+)+e \rightarrow H_2^{+*} \rightarrow H^+ + H^*.$$

However, since we rely primarily on experimental data, when possible, we have automatically included these contributions.

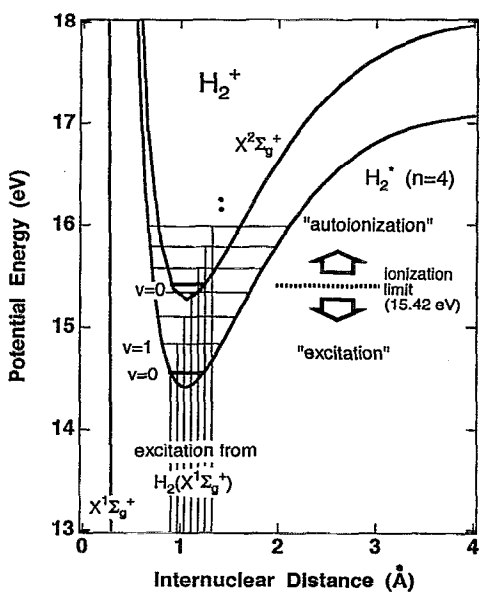

FIG. 16. The cross section for ionization to the $v=0$ molecular ion is related to the cross section for excitation to $v=0$, $n=4$ taken as an example, Rydberg molecule. Excitation to higher vibrational level than that of the ground vibrational state of the molecular hydrogen ion results in autoionization. In our model the sum of the excitation cross sections to the nonautoionizing vibrational levels, $v=0$, 1, 2, and 3 in this example denoted by "excitation," is adopted for the excitation cross section to the $n=4$ level.

[1] T. Fujimoto, K. Sawada, and K. Takahata, J. Appl. Phys. **66**, 2315 (1989).
[2] T. Fujimoto, K. Sawada, K. Takahata, K. Eriguchi, H. Suemitsu, K. Ishii, R. Okasaka, H. Tanaka, T. Maekawa, Y. Terumichi, and S. Tanaka, Nucl. Fusion Lett. **29**, 1519 (1989).
[3] T. Fujimoto, J. Phys. Soc. Jpn. **47**, 273 (1979).
[4] K. Sawada, K. Eriguchi, and T. Fujimoto, J. Appl. Phys. **73**, 8122 (1993).
[5] T. E. Sharp, At. Data **2**, 119 (1971).
[6] W. T. Miles, R. Thompson, and A. E. S. Green, J. Appl. Phys. **43**, 678 (1972).
[7] S. Chung and C. C. Lin, Phys. Rev. A **17**, 1874 (1978).
[8] S. E. Branchett, J. Tennyson, and L. A. Morgan, J. Phys. B **23**, 4625 (1990).
[9] D. R. Bates, A. E. Kingston, and R. W. P. McWhirter, Proc. R. Soc. London **267**, 297 (1962).
[10] D. R. Bates and A. E. Kingston, Planet. Space Sci. **11**, 1 (1963).
[11] R. W. P. McWhirter and A. G. Hearn, Proc. Phys. Soc. **82**, 641 (1963).
[12] B. Adamczyk, A. J. H. Boerboom, B. L. Schram, and J. Kistemaker, J. Chem. Phys. **44**, 4640 (1966).
[13] A. Crowe and J. W. McConkey, J. Phys. B **6**, 2088 (1973).

[14] D. Rapp and P. Englander-Golden, J. Chem. Phys. **43**, 1464 (1965).
[15] R. K. Janev, W. D. Langer, K. Evans, and D. E. Post, *Elementary Processes in Hydrogen–Helium Plasma, Cross Sections and Reaction Rate Coefficients* (Springer, Berlin, 1987).
[16] H. Nishimura and A. Danjo, J. Phys. Soc. Jpn. **55**, 3031 (1986).
[17] A. W. Fliflet and V. McKoy, Phys. Rev. A **21**, 1863 (1980).
[18] S. Chung and C. C. Lin, Phys. Rev. A **12**, 1340 (1975).
[19] M. A. P. Lima, T. L. Gibson, and V. McKoy, Phys. Rev. A **38**, 4527 (1988).
[20] K. L. Baluja, C. J. Noble, and J. Tennyson, J. Phys. B **18**, L851 (1985).
[21] B. I. Schneider and L. A. Collins, Phys. Rev. A **33**, 2982 (1986).
[22] T. N. Rescigno and B. I. Schneider, J. Phys. B **21**, L691 (1988).
[23] M. A. P. Lima, T. L. Gibson, W. M. Huo, and V. McKoy, J. Phys. B **18**, L865 (1985).
[24] S. A. Cohen, in *Physics of Plasma-Wall Interactions in Controlled Fusion* (Plenum, New York, 1986), p. 733.
[25] J. R. Hiskes, Notas Fis. **5**, 348 (1982).
[26] C. Gorse, M. Capitelli, J. Bretagne, and M. Bacal, Chem. Phys. **93**, 1 (1985).
[27] J. M. Bardsley and J. M. Wadehra, Phys. Rev. A **20**, 1398 (1979).
[28] J. R. Hiskes, J. Appl. Phys. **51**, 4592 (1980).
[29] H. Tawara, Y. Itikawa, H. Nishimura, and M. Yoshino, J. Phys. Chem. Ref. Data **19**, 617 (1990).
[30] R. Celiberto, M. Cacciatore, M. Capitelli, and C. Gorse, Chem. Phys. **133**, 355 (1989).
[31] J. R. Hiskes, AIP Conf. Ser. **287**, 155 (1992).
[32] T. N. Rescigno and B. I. Schneider, J. Phys. B **21**, L691 (1988).
[33] R. Celiberto and T. N. Rescigno, Phys. Rev. A **47**, 1939 (1993).
[34] J. R. Hiskes, J. Appl. Phys. **70**, 3409 (1991).
[35] M. Cacciatore and M. Capitelli, Chem. Phys. **55**, 67 (1981).
[36] M. Cacciatore, M. Capitelli, and C. Gorse, J. Phys. D **13**, 575 (1980).
[37] R. Celiberto, M. Capitelli, and M. Cacciatore, Chem. Phys. **140**, 209 (1990).
[38] A. C. Allison and A. Dalgarno, At. Data **1**, 289 (1970).
[39] A. Dalgarno and T. L. Stephens, Astrophys. J. **160**, L107 (1970).
[40] M. Glass-Maujean, At. Data Nucl. Data Tables **30**, 273 (1984).
[41] R. E. Imhof and F. H. Read, J. Phys. B **4**, 1063 (1971).
[42] L. C. Johnson, Astrophys. J. **174**, 227 (1972).
[43] S. K. Srivastava and S. Jensen, J. Phys. B **10**, 3341 (1977).
[44] J. M. Ajello, S. K. Srivastava, and Y. L. Yung, Phys. Rev. A **25**, 2485 (1982).
[45] D. E. Shemansky and J. M. Ajello, J. Geophys. Res. **88**, 459 (1983).
[46] J. M. Ajello, D. Shemansky, T. L. Kwok, and Y. L. Yung, Phys. Rev. A **29**, 636 (1984).
[47] M. A. Khakoo and S. Trajmar, Phys. Rev. A **34**, 146 (1986).
[48] F. J. de Heer and J. D. Carriere, J. Chem. Phys. **55**, 3829 (1971).
[49] E. J. Stone and E. C. Zipf, J. Chem. Phys. **56**, 4646 (1972).
[50] G. P. Arrighini, F. Biondi, C. Guidotti, A. Biagi, and F. Marinelli, Chem. Phys. **52**, 133 (1980).
[51] L. Mu-Tao, R. R. Lucchese, and V. McKoy, Phys. Rev. A **26**, 3240 (1982).
[52] M. J. Redmon, B. C. Garrett, L. T. Redmon, and C. W. McCurdy, Phys. Rev. A **32**, 3354 (1985).
[53] T. N. Rescigno, C. W. McCurdy, V. McKoy, and C. F. Bender, Phys. Rev. A **13**, 216 (1976).
[54] D. E. Shemansky, J. M. Ajello, and D. T. Hall, Astrophys. J. **296**, 765 (1985).
[55] J. M. Ajello, D. E. Shemansky, and G. K. James, Astrophys. J. **371**, 422 (1991).
[56] T. Fujimoto and R. W. McWhirter, Phys. Rev. A **42**, 6588 (1990).
[57] J. W. McGowan, M. A. Fineman, E. M. Clarke, and H. P. Hanson, Phys. Rev. **167**, 52 (1968).
[58] R. S. Berry, J. Chem. Phys. **45**, 1228 (1966).
[59] H. Takagi and H. Nakamura, J. Chem. Phys. **74**, 5808 (1981).
[60] B. Peart and K. T. Dolder, J. Phys. B **4**, 1496 (1971).
[61] B. Peart and K. T. Dolder, J. Phys. B **5**, 860 (1972).
[62] C. J. Latimer, A. D. Irvine, M. A. McDonald, and O. G. Savage, J. Phys. B **25**, L211 (1992).
[63] C. J. Latimer, K. F. Dunn, N. Kouchi, M. A. McDonald, V. Srigengan, and J. Geddes, J. Phys. B **26**, L595 (1993).